Response to comments by Referee 1

First of all we would like to thank you for all the comments. This reply provides answers/discussion of the comments. The text in blue represents changes and additions made to the paper.

(1) "*Currently it is stated that the parametrization from Dunne et al. (2016) is expanded to lower sulfuric acid concentrations and higher ion concentrations. This is an overstatement since Dunne et al. explored new particle formation for a wide range of sulfuric acid, ammonia, temperature and ion concentrations. However, the present study examined NPF at only one temperature (295 K) and one ammonia equivalent mixing ratio of 2200 pptv. For these conditions, the sulfuric acid and ion concentrations were varied. Given the fact that the authors did not resolve the chemistry of the nucleating clusters, it is also speculative that NH3 is the only possibility of explaining the high NPF rates at low sulfuric acid. In principle, other contaminants (e.g. organics or amines) could probably also explain the data. Therefore, without having identified the chemistry of the nucleating clusters the statements about the chemical parameter space that the current study explores need to be reformulated*"

We will make sure to clarify that we only expand the parametrization from Dunne et al. (2016)/Gordon et al. (2017) at a temperature of 295 K and ammonia equivalent mixing ratio of 2200 pptv. We will also stress that it is not only NH_3 that explains the high NPF rates since the amount of other contaminants is unknown. We will rephrase some statements about the ternary nucleation rates to clarify that the nucleation pathways in this study are unknown. See specific comments further down.

(2)"*The results presented in figure 6 are not in agreement with previous studies. At 2e+07 cm^{-3} of sulfuric acid, the contribution from binary neutral nucleation to the total neutral nucleation rate is as high as the contribution from the other channels (binary ion-induced, ternary neutral and ternary ion-induced). For this warm temperature, it is impossible that binary neutral nucleation yields a formation rate of ∼0.04 cm-3 s-1 (at sulfuric acid of 2e+07 cm^{-3}) since the clusters evaporate too rapidly (see, e.g., Hanson and Lovejoy, 2006; Ehrhart et al., 2016; Duplissy et al., 2016). At these conditions, binary neutral nucleation should be completely negligible and even the binary ioninduced component should be negligible compared to the ternary channels (Ehrhart et al., 2016; Duplissy et al., 2016). Therefore, a re-evaluation of the different nucleation channels is necessary as well as a more thorough inter-comparison to previous studies. Given the presented results and the results from previous studies it seems very likely that the nucleation rates presented are by far dominated by the ternary channel.*"

We have rewritten the evaluation of the nucleation channels to ensure consistency with results from previous studies and included a table for inter-comparison (see below and Sect. 4 in paper). We have left out Figure 6 and the fit. Finally we have emphasized that our results should be seen more as an expansion of the Dunne et al./Gordon et al. parametrization to higher ionization levels (for the investigated parameters) than a separate parametrization. See specific comments further down.

It can be complicated to compare different experimental studies, even under similar conditions, because it is unclear how experimental techniques and parameters affect the results. Four studies (Kirkby et al., 2011; Almeida et al., 2013; Duplissy et al., 2016; Kürten et al., 2016), all performed in the European Organization for Nuclear Research CLOUD (Cosmics Leaving Outdoor Droplets) chamber are most relevant for inter-comparison, because they were made in a reaction chamber analogous to this study. The experiments presented in Sipilä et al. (2010) were performed in a flow tube. Yet, we include these in the comparison, because in it nucleation was measured directly at the critical cluster size with a PSM instrument. Table 1 gives an overview of the studies and conditions that were compared. Some studies consist of several experiments using varying parameters. Table 1 only shows the measurements made under conditions that match the parameters of this study. The experiments from this study with lowest ionization are used for comparison, because this ionization level (4.4 cm^{-3} s^{-1}) is close to the cosmic ray background ionization (GCR $\sim$ 3 cm^{-3} s^{-1}).

Table 1. Comparison of similar nucleation rate experiments. The numbers refer to the different studies: 1: This study, 2: Kirkby et al. (2011), 3: Almeida et al. (2013), 4: Duplissy et al. (2016), 5: Kürten et al. (2016) ,6: Sipilä et al. (2010). The fifth parameter, D, is the mobility diameter. GCR corresponds to the background GCR (Galactic Cosmic Ray) ionization ($\sim$ 3 cm^{-3} s^{-1}). Cells with a - mean that the value was not measured or reported.

	1	2	3	4	5	6
H_2SO_4 [cm^{-3}]	$4 \cdot 10^6$ - $3 \cdot 10^7$	$2 \cdot 10^8$ - $1 \cdot 10^9$	$7 \cdot 10^6$ - $3 \cdot 10^8$	$5 \cdot 10^8$ -$8 \cdot 10^8$	$1 \cdot 10^8$ - $2 \cdot 10^8$	$2 \cdot 10^6$-$2 \cdot 10^8$
T [K]	295	292	278	299	292	293
RH	38%	38 %	38 %	36%	38%	22%
q [cm^{-3} s^{-1}]	4.4	GCR	GCR	GCR	GCR	GCR
D [nm]	1.4	1.7	1.7	1.7	1.7	$\sim 1.3 - 1.5$
NH_3	-	<35 ppt	2-250 ppt	-	1400 ppt	-[†]
J [cm^{-3} s^{-1}][⋆]	0.002-1	0.005-30	0.003-25	0.01 - 1	3-10	1-1000

[⋆] The nucleation rates are read of the figures in the respective papers and are therefore only approximate values. [†] The observed growth rate in this study was close to that from pure sulphuric acid.

From Table 1 it is clear that experiments conducted under the exact same conditions as in this study do not exist. Nevertheless, the nucleation rates in this study lie slightly below or within the range of the nucleation rates obtained in the experiments performed in the CLOUD chamber (studies 2-5). Except for study 3, which was made under lower temperatures, these studies have around one to two orders of magnitude higher sulphuric acid concentrations than is the case for this study. As with the parametrization this indicates the existence of other nucleating species within our chamber. By comparing study 2 and 5 made under almost identical conditions the effect on nucleation of an increase in NH_3 concentration is evident (e.g at [H_2SO_4]=2 $\cdot 10^8$ cm^{-3} which is the lower limit for study 2 and the upper limit for study 5).

The model of binary nucleation presented in Ehrhart et al. (2016) shows good agreement with measurements performed in the CLOUD chamber at lower temperatures (<273 K). However at tropospheric temperatures (>273 K) the binary nucleation rate cannot explain the nucleation rates that are observed in either of these studies at the given sulphuric acid concentrations. In particular not for the low tropospheric concentrations in this study. Ehrhart et al. (2016) attributes the differences to contamination which is more important in providing stabilization for the pre-nucleating clusters when the temperature and thereby evaporation is high.

(3) "*Regarding the identification of the relevant nucleation scheme, one possibility would be to use the CI-APi-TOF as an APi-TOF. This should indicate what fraction of sulfuric acid cluster ions contains ammonia molecules (or any other contaminants); based on Schobesberger et al. (2015) it might also be possible to derive an estimate of the ammonia contaminant level. Given the fact that the experiments were made at high ion concentrations, the APi-TOF should yield strong signals, which would shine a light on the nucleation pathway.*"

This is an interesting idea for future studies that we will keep in mind. Especially the idea from Schobesberger et al. of using the the ratio of NH_3 to H_2SO_4 in the clusters to determine the corresponding concentration ratio. Unfortunately we cannot redo the experiments at the present.

(4)"*The data evaluation process needs to be explained in more detail. Especially, an additional figure should be added that shows the time development of particle concentration, UV light intensity, H2SO4 concentration, temperature, etc. Based on that figure it should be explained over what period the data for the derivation of J were averaged.*"

We will provide the requested figure and include an explanation of the experimental run sequence and a more in depth description of the data analysis possibly including a correction to the nucleation rate. See specific comments further down.

Specific comments

1) "*p. 1, l. 10/11 (abstract): the parameter space is only extended for one NH3 concentration and one temperature (1.2 ppbv and 295 K, see Fig. 4)*"

We changed the phrasing in the abstract:

One hundred and ten direct measurements of aerosol nucleation rate at high ionization levels were performed in an 8 m^3 reaction chamber. Neutral and ion-induced particle formation from sulphuric acid (H_2SO_4) as a function of ionization and H_2SO_4 concentration was studied. Other species that could participate in the nucleation, such as NH_3 or organic compounds, were not measured but assumed constant and the concentration was estimated based on the parametrization by Gordon et al. (2017). Our parameter space is thus: [H_2SO_4]=$4 \cdot 10^6$ - $3 \cdot 10^7$ cm^{-3}, [NH_3+ org]=2.2 ppb, T=295 K, RH=38%, and ion concentrations of 1700 - 19000 cm^{-3}. The ion concentrations, which correspond to levels caused by a nearby supernova, were achieved with gamma ray sources. Nucleation rates were directly measured with a particle size magnifier (PSM Airmodus A10) at a size close to critical cluster size (mobility diameter of ~1.4 nm) and formation rates at mobility diameter of ~4 nm were measured with a CPC (TSI model 3775). The measurements show that nucleation increases by around an order of magnitude when the ionization increases from background to supernova levels under fixed gas conditions. The results expand the parametrization presented in Dunne et al. (2016) and Gordon et al. (2017) (for [NH_3+org]=2.2 ppb and T=295 K) to lower sulphuric acid concentrations and higher ion concentrations. The results make it plausible to expand the parametrization presented in Dunne et al. (2016) and Gordon et al. (2017) to higher ionization levels.

2) "*p. 2, l. 1: further references regarding the influence of organics on NPF should be added (e.g., Zhang et al., 2004; Ehn et al., 2014; Kirkby et al., 2016)*"

The mentioned references were added:

... Nucleation can be significantly enhanced by other substances, the dominant ones being ammonia (NH_3) and organic molecules (Kirkby et al., 2011; Dunne et al., 2016; Zhang et al., 2004; Ehn et al., 2014; Kirkby et al., 2016).....

3) "*p. 2, l. 9: add "The" at the beginning of the sentence*"

Added "The":

The typical concentration range..

4) "*p. 2, l. 10: replace "outlet" with "emissions"*"

Replaced it:

The concentrations vary with location, time of the day and emission of SO_2, which can be both anthropogenic and natural.

5) "*p.2, l. 31/32: Where did the air originate from? Was it from gas bottles, from a dewar or was an (ambient) air purification system used? If a gas purification system was used, what measures were taken to clean the gas? Later in the paper it is concluded that the contamination of ammonia was quite high (1.2 ppbv); therefore, it would be good to know if and how it was attempted to minimize the ammonia contamination.* "

The following has been added to the experimental methods. Also note that the estimated NH_3 concentration is not "true NH_3" since this amount can also include organics, as we unfortunately are not able to distinguish between these.

Dry purified air (20 L/min) from a compressor with an active charcoal, citric acid, and particle filter was passed through a humidifier and added to the chamber to reach a relative humidity of 38%. 5 L/min of dry air from the same compressor went through an ozone generator where O_2 is photolyzed by a UV lamp to produce O_3. Sulphur dioxide (3.5 mL/min) was added from a pressurized bottle (5 ppm SO_2 in air, AGA). The resulting concentrations of O_3 and SO_2 were measured by a Teledyne T400 analyzer and SO_2 with a Thermo 43 CTL analyzer, respectively.

6) "*p. 3, l. 5: Temperature has a strong influence on NPF (see e.g. Ehrhart et al., 2016). How was the temperature held constant at 295 K? Was there any increase in temperature when the UV light was turned on? If yes, by how much did the temperature increase?*"

The temperature in the laboratory is regulated and held stable by an external ventilation system thereby keeping the temperature in the chamber stable. Figure 1 (Figure 3 in the paper) shows, among other things, the temperature during an experimental run. The temperature-increase caused by the UV lamps varied from $\sim$ 0.05 K to 0.2 K when the UV lamps were on 15% to 45 % power respectively. Figure 1 shows the experimental run for 22% UV, and in this case the temperature increased by $\sim$ 0.1 K. This increase should be negligible ($\sim$5% for the 0.2 K change based on Dunne et al. (2016)) when it comes to nucleation rates. The discussion of this is added to the explanation of the experimental run sequence.

7) "*p. 4, l. 7: "irradiation" instead of "radiation"*"

Thanks:

To achieve a homogeneous irradiation of the chamber, ...

8) "*p. 5, Figure 2: What is meant by "average ionization" for the left panel of the figure? What is the unit?*"

Both panels in Figure 2 two the same type of Geant4 simulation but for two different shielding thicknesses (left: 0 cm, right: 8.5 cm). The figures show the ionization rate in the unit [$cm^{-3}s^{-1}$] throughout the chamber. This value depends on distance to the gamma sources. The average ionization is the average for the entire chamber calculated by Geant4 and given as an output parameter from the simulation, the unit is still [$cm^{-3}s^{-1}$]. To make this as clear as possible we have added this to the captions of both Figure 2 and Table 1 and to the text:

There is some circulation of the air in the chamber and the air is sampled from approximately in the middle between the sources as seen in Fig. 1, therefore it is assumed that the average ionization for the entire chamber is a good representation of the ionization of the sampled air.

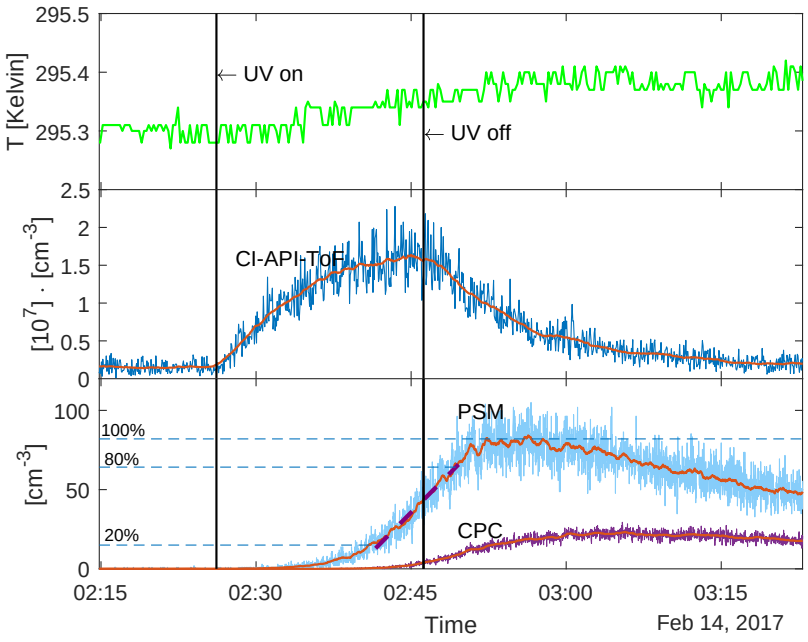

Figure 1. Run sequence for an experiment with 22% UV and N=8400 [cm^{-3}]. The vertical lines show when the UV lamps were turned on and off. Top panel: Temperature in the chamber. Middle panel: H_2SO_4 concentration measured with the CI-API-ToF and 50 point moving average shown in red. Bottom panel: Aerosol particle concentration measured with PSM and CPC (before the loss correction). The 50 point moving average is shown in red. The purple dashed line shows the linear fit between 20 and 80 of the maximum concentration. The gradient of this fit (made on the loss-corrected data) was used as the nucleation rate.

9) "*p. 5, l. 9 ff. (section 2.2): The authors need to add a figure that shows the time development of [H2SO4], particle concentration, UV light and temperature; based on that figure the experimental run sequence should be explained.*"

We added the figure (see Fig. 1 in this, and Fig. 3 in the article) and explained the experimental run sequence:

Figure **??** shows an example of a run sequence (for 22% UV and N=8400 [cm^{-3}]) as a function of time. The UV lamps were turned on for twenty minutes from 02:26:10 to 02:46:12. The top panel shows the temperature in the chamber during the experiment. It shows that the temperature increased by ∼0.1 K when the UV lamps were turned on. When the UV was on the highest setting (45%) the temperature increased by 0.2 K. This slight increase in temperature is negligible in regards to the nucleation rate (5% change for a 0.2 K increase at the highest [H_2SO_4] based on Dunne et al. (2016)). Therefore, a constant temperature of 295.4 K was used in the further analysis. The second panel shows the H_2SO_4 concentration in units of 10^7 [cm^{-3}]. The red line is the 50 point boxcar moving average. Immediately after the UV lamps were turned on, the H_2SO_4 concentration started to increase. When the UV was turned off, the H_2SO_4 was lost to scavenging by aerosol particles and to the chamber walls. The third panel shows the aerosol particle concentration measured with the PSM and CPC without any corrections for the wall-losses. The red lines represent the 50 point boxcar moving average which is used for the further data analysis to avoid artefacts from noise. Corrections for particle loss to chamber walls are presented further down and the data analysis was performed on the corrected version of the moving average.

10) "*p. 6, l. 21: please mention the detection limit for the sulfuric acid measurements.*"

We realize that the original phrasing is confusing and rewrite the sentence from:

The lower limit of the H_2SO_4 concentrations was chosen based on the detection limit of the instrument. The CPC with cut-off diameter of 4 nm was the limiting instrument because the majority of the particles are lost during the growth from 1.4 to 4 nm.

to:

The lower limit of the H_2SO_4 concentrations was chosen based on the particle detection limit of the CPC model 3775, which was the limiting instrument because the majority of the particles are lost during the growth from 1.4 to 4 nm.

11) "*p. 6, l. 3 (something is wrong with the line numbering): "drifts" instead of "drift"*"

OK:

..to avoid unnoticed drifts in parameters...

12) "*p. 7, l. 18: The reference to Hansen (2016) refers to a bachelor's thesis, which I couldn't find on the internet. The authors need to summarize how the mentioned corrections were made. In addition, it is not clear why the H2SO4 was not derived from the signal related to the exact mass of HSO4-. The CI-APi-TOF has a mass resolving power that is high enough to discriminate HSO4- from most other isobaric signals. The commonly used data evaluation tools for CI-APi-TOF data (Toftools and Tofware) also allow the subtraction of noise. Therefore, it is not clear why this software has not been used.*"

In Hansen 2016 sulphuric acid data analyzed with Tofware was compared to an analysis of the "raw " ($\pm$ 0.5 AMU) data from TofDaq. The relation between those two datasets was found to vary between 1.24 and 1.27 for a sulphuric acid concentration range between 0.6e7 and 1.6e7 cm-3 over 8 days of stable measurements. Since it is much faster to analyse the TofDaq-generated hdf-files directly (we have 2 months of 4-hour files) we have chosen this approach as it does not increase the uncertainty in the measurement much. For detalied peak analysis Tofware or Toftools would certainly be required.

We have changed the sentence referencing this work to the following:

This was also taken into account and corrected for using the results from Hansen 2016 where the relation between analysis of the $\pm$ 0.5 AMU data from the API-ToF and data analyzed using Tofware (Stark et al., 2015) was found.

13) "*p. 7, l. 4: The retrieval of the "mean peak concentration" should be demonstrated in a figure. The whole data evaluation process needs to be described in more detail.*"

Figure 1 (Fig. 3 in the paper) is used to describe the data evaluation process, including the retrieval of the mean peak concentration. In addition we have clarified in the text that the statistical uncertainty in the sulphuric acid is calculated from the std-error of the difference between the measured data and the smoothed data.

The H_2SO_4 concentration is determined from the peak value of the 50 point boxcar moving average (the red line in Figure 3). This method introduces a statistical uncertainty in addition to the uncertainty in the calibration factor. The

statistical uncertainty arises from the fluctuations in the non-smoothed data and was calculated from the standard error of the difference between the non-smoothed and the smoothed data for the 50 points around the peak.

14) "*p. 7, l. 20/21: The GRs are indeed very high given the rather low sulfuric acid concentrations. The theoretical approach from Nieminen et al. (2010) indicates that a sulfuric acid concentration of 1.5e+07 cm-3 results in a GR of ∼1 nm/h (with GR being linearly dependent on H2SO4) for the binary system. This relationship has been found to be consistent with measured data (Lehtipalo et al., 2016). Therefore, the expected GR for the sulfuric acid range relevant for this study would be 0.5 to 2 nm/h, i.e., a factor of ∼20 lower than what has been measured.*"

As seen in the discussion the high GR can be caused by the participation of oxidized organics.

15) "*p. 8, l. 22/23: The authors attribute the fast growth of the particles to the presence of highly oxidized molecules. However, if these compounds dominate the GR (see previous comment) a fraction of them should also be capable of enhancing the particle formation rates (see Kirkby et al., 2016). Discussion about the possibility of explaining the high formation rates due to organics should be added.*"

We have mentioned that the high nucleation rates could be caused by the participation of organics.

These other vapours can also contribute to the observed nucleation rates (See Sect. 4 Results and Discussions).

In addition we have included more thorough discussion of the relatively high nucleation rates found in this study (See Sect. 4 Results and Discussion).

16) "*p. 8, l. 27-29: Again, it would be good to show a figure that indicates the range over which the gradient dN/dt was calculated. In addition, the equation for determining the particle formation rates neglects some potential corrections: In the calculation, all particles larger than the cut-off diameter of 1.4 nm are considered. However, the particles beyond that size are subject to loss processes such as wall loss, dilution and coagulation. These processes lower the measured particle number density to some degree (see Kulmala et al., 2012). In fact, the authors write that the majority or particles is lost during their growth from 1.4 to 4 nm (p. 6, l. 22); in this case the loss terms definitely need to be taken into account in the calculation of J. In addition, a mobility diameter of 1.4 nm is quite small. The results from Duplissy et al. (2016) indicate that the critical size can be significantly larger at warm temperature. Are the authors sure, that 1.4 nm is at or above the critical size?* "

The newly added Figure 1 (Figures 3 and 4 in the paper) indicates the range over which the gradient was calculated. And we have added references to the figure in the discussion of the data processing. Regarding the loss correction term, we argued that since we measure at a size very close to the critical size the loss term is negligible. However, we have now added a loss-term and corrected all of our measurements. The loss term is calculated as follows:

From Svensmark et al. (2013) we have the size-dependent loss term k which is an approximation of particle loss to the chamber walls:

$$k = \lambda / r_i^{\gamma} \tag{1}$$

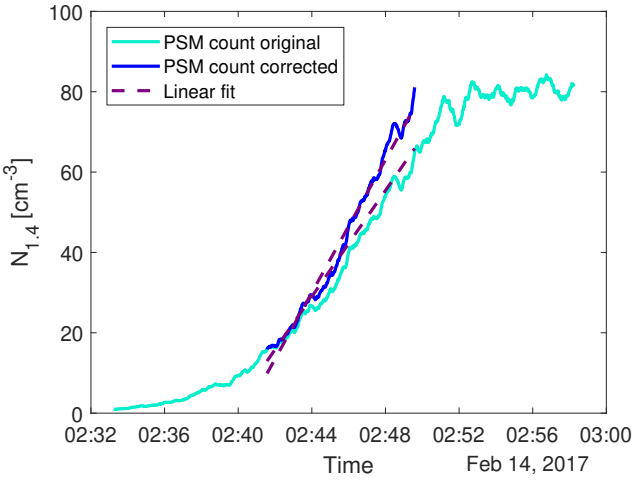

Figure 2. An example of the original particle count from the PSM and the corrected. The red dashed lines show the linear fit for both data sets. The linear fit from the corrected data is used to determine the nucleation rate.

The term γ is detemined experimentally, in Svensmark et al. (2013), to $\gamma = 0.69 \pm 0.05$ and $\lambda = 6.2 \cdot 10^{-4}$ nm$^{\gamma}$s^{-1}. The average radius r_i that the particles have at a certain time is given by the critical radius (when they were measured by the PSM) the growth rate and the time they had to grow in, this is multiplied by 0.5 to get the average size:

$$r = 0.7nm + GR \cdot 0.5 \cdot \Delta t \tag{2}$$

The loss term is used to correct the particle count from the PSM at any time:

$$N_{corrected} = N_{PSM}/exp(-k\Delta t) \tag{3}$$

The figure below shows an example of the original count, the corrected count and the linear fit used to determine dN/dt. both prior and after the correction.

See section 3.3 for the revised version of the "Determination of the nucleation rate".

Finally, you ask if we are sure that 1.4 nm is above the critical size at this temperature. No, we are not sure, but since this is the cut-off size of the PSM, which is also determined with some uncertainty, and it is close to the value used in Dunne et al. (2016), we choose to assume this.

17) "*p. 8, l. 32: The systematic uncertainty of 5% for the H2SO4 measurements is quite low. How was this value derived?*"

This is the uncertainty in the final measurement. There are additional uncertainties in the parameters used in the calibration, which amount to about 33% (Kürten et al., 2012). We've changed the sentence to reflect this:

"and the calibration uncertainty for the mass spectrometer (5% measurement error + additional errors from calibration parameters (30%, Kürten et al. (2012)))."

18) "*p. 10, l. 9: The experimental data were fitted to functions representing binary nucleation (neutral and ion-induced, eq. (4) and (5)). However, from Dunne et al. (2016) it can be concluded that nucleation is almost entirely dominated by the ternary nucleation terms (J_{tn} and J_{ti}) at 295 K (sulfuric acid between 7e+06 and 3e+07, [ion] = 1700 cm-3) if ammonia is present at 1.2 ppbv. Therefore, the use of binary nucleation to represent and fit the data (Fig. 5) is not justified (see also comment above). In addition, the parameters provided by Dunne et al. (2016) do not have high enough precision in order to replicate their measured data; therefore, the higher precision values provided by Gordon et al. (2017) should be used for calculating the individual components of the nucleation channels.*"

We admit to having overlooked the conclusion that the ternary nucleation terms completely dominate at the given gas concentrations and temperature. Therefore we remove the fit and discussion of the binary channels and focus on the ternary channels. We leave out the fitting of our own parametrization as it does not make sense to fit the binary terms, when they are negligible. On the other hand we do not have measurements of ternary contaminants and therefore do not fit the ternary channels either. In stead, we simply compare our results with the parametrisation presented in Gordon et al. (2017) which has higher precision parameters than the ones we used previously. The new parameters and the addition of the loss correction result in slightly higher nucleation rates than in the previous version of the paper. Therefore the amount of contamination from NH_3 and organic species had to be adjusted and is now $\sim$ 2.2 ppb in ammonia equivalent concentration. The results are seen in Figure 4/5 and the discussion is added to the "Results and Discussion" section.

19) "*p. 10, l. 15: "n-" instead of "N"?*"

Yes, you are right, however, as this section is removed it is no longer relevant.

20) "*p. 11, Fig. 5: something seems to be wrong with the fit curves, e.g., the yellow line separates the yellow symbols such that 2 points are above the line and 9 points are below the line. For the blue curve, the situation is similar, which should not be the case if all points are weighted equally.*"

The points were not weighted equally, but according to the standard deviation in the data. Since the fit and this figure is left out, it is no longer relevant.

19) "*p. 12, l. 26: "suggests" and p. 12, l. 27: "were"*"

As this section is removed it is no longer relevant.

Response to comments by Referee 3 (Brian Thomas)

Thank you for your comments. The following presents our response to the specific comments. The text in blue represents changes and additions made to the paper.

1) *"They say O3 was added to the experiment chamber. Why is that? I did not find an explanation of why this was done, or the concentration added. It is important to consider what effect O3 may have on the processes involved. "*

O_3 was added to allow for formation of H_2SO_4 via photolysis by UV light. The concentration was between 20-30 ppb which corresponds to concentrations in the lower troposphere. Apart from the photolysis ozone could oxidize eventual organic impurities in the chamber which may participate in the cluster formation similarly to how it happens in the atmosphere (Dunne et al. 2016). We have mentioned the concentration of O_3 in the new version of the paper along with

the concentration of SO_2:

5 L/min of dry air from the same compressor went through an ozone generator where O_2 is photolyzed by a UV lamp to produce O_3 . Sulphur dioxide (3.5 mL/min) was added from a pressurized bottle (5 ppm SO_2 in air, AGA). The resulting concentrations of O_3 (20-30 ppb) and SO_2 (0.6-0.9 ppb) were measured by a Teledyne T400 analyzer and with a Thermo 43 CTL analyzer, respectively.

2) *"Similarly, they say the pressure was held at 0.1 mbar. This is very low pressure compared to atmospheric pressure in the lower and even middle atmosphere."*

We state that the pressure was held at 0.1 mbar overpressure, and realize that this is not expressed clearly enough. We have rephrased this to the following:

The pressure was held at a standard pressure of $\sim$ 1 bar with a slight (0.1 mbar) overpressure relative to the surroundings, the temperature at 295 K and the UV intensity was varied as part of the experiments.

3) *"Likewise, they say the temperature was held at 295 K, which is relatively high compared to that in most of the atmosphere above ground level. These choices need to be explained. "*

It would be preferable to perform the experiments under varying temperatures, however, due to lack of equipment and time constraints this was not possible. A temperature of 295 K is relevant for the lower troposphere. In addition, this temperature is close to one of the temperatures used in the study by Dunne et al. (2016). Since we compare our results with this study and use our results to expand their parametrization we consider 295 K to be an appropriate temperature. We now discuss this in the paper (see below).

4) *"I found one typo; on page 12, in the next-to-last paragraph of section 4, "where" should be "were" in the sentence "When the experiments where fitted. . ."*"

Thank you. It has been corrected.

5) *If you can say something about the possible variation with temperature that would be good, since 295K really only is realistic for ground level and the very lower troposphere, which seems less relevant for your study. I understand the experimental constraint (and the connection to Dunne), but I do think you should say whatever you can about the possible effect of lower temperature. Similarly for pressure.*

The following discussion on the effect of temperature on nucleation was added:

The temperature used in this paper is only relevant to the boundary layer of the troposphere. At this high temperature evaporation of pre-nucleation clusters is very important and the stabilization provided by ions can have a strong effect (Lovejoy et al., 2004) as is also seen in this study. Higher in the troposphere where temperatures are colder the importance of evaporation decreases. However ions can still have a strong effect on the nucleation rates. Kirkby et al. (2011) showed that ions can affect pure binary nucleation rates at mid-troposphere conditions ($\sim$ 250 K). An even higher increase in ionization, as used in this work, would increase the nucleation rates even more - by about one order of magnitude according to the parametrization used here. The concentrations of ternary gases is also expected to be lower in the free troposphere, which increases the effect of the ions.

References

Almeida, J. et al.: Molecular understanding of sulphuric acid–amine particle nucleation in the atmosphere, Nature, 502, https://doi.org/doi:10.1038/nature12663, 2013.

Dunne, E. M., Gordon, H., Kürten, A., et al.: Global atmospheric particle formation from CERN CLOUD measurements, Science, 354, 1119–1124, https://doi.org/10.1126/science.aaf2649, http://science.sciencemag.org/content/354/6316/1119, 2016.

Duplissy, J., Merikanto, J., Franchin, A., Tsagkogeorgas, G., Kangasluoma, J., Wimmer, D., Vuollekoski, H., Schobesberger, S., Lehtipalo, K., Flagan, R., et al.: Effect of ions on sulfuric acid-water binary particle formation: 2. Experimental data and comparison with QC-normalized classical nucleation theory, Journal of Geophysical Research: Atmospheres, 121, 1752–1775, 2016.

Ehn, M. et al.: A large source of low-volatility secondary organic aerosol, Nature, 506, https://doi.org/doi:10.1038/nature13032, 2014.

Ehrhart, S., Ickes, L., et al.: Comparison of the SAWNUC model with CLOUD measurements of sulphuric acid-water nucleation, Journal of Geophysical Research: Atmospheres, 121, 12,401–12,414, https://doi.org/10.1002/2015JD023723, http://dx.doi.org/10.1002/2015JD023723, 2015JD023723, 2016.

Gordon, H., Kirkby, J., Baltensperger, U., et al.: Causes and importance of new particle formation in the present-day and preindustrial atmospheres, Journal of Geophysical Research: Atmospheres, 122, https://doi.org/10.1002/2017JD026844, 2017.

Kirkby, J., Curtius, J., Almeida, J., Dunne, E., et al.: Role of sulphuric acid, ammonia and galactic cosmic rays in atmospheric aerosol nucleation, Nature, 476, 429–433, https://doi.org/10.1038/nature10343, 2011.

Kirkby, J., Duplissy, J., Sengupta, K., et al.: Ion-induced nucleation of pure biogenic particles, Nature, 533, https://doi.org/doi:10.1038/nature17953, 2016.

Kürten, A., Bianchi, F., Almeida, J., et al.: Experimental particle formation rates spanning tropospheric sulfuric acid and ammonia abundances, ion production rates, and temperatures, Journal of Geophysical Research: Atmospheres, 121, 12,377–12,400, https://doi.org/10.1002/2015JD023908, http://dx.doi.org/10.1002/2015JD023908, 2015JD023908, 2016.

Kürten, A., Rondo, L., Ehrhart, S., and Curtius, J.: Calibration of a Chemical Ionization Mass Spectrometer for the Measurement of Gaseous Sulfuric Acid, J. Phys. Chem. A, 116, 6375–6386, https://doi.org/doi:10.1021/jp212123n, 2012.

Lovejoy, E. R., Curtius, J., and Froyd, K. D.: Atmospheric ion-induced nucleation of sulfuric acid and water, Journal of Geophysical Research (Atmospheres), 109, 1–11, https://doi.org/10.1029/2003JD004460, 2004.

Sipilä, M., Berndt, T., Petäjä, T., Brus, D., Vanhanen, J., Stratmann, F., Patokoski, J., Mauldin, R. L., Hyvärinen, A.-P., Lihavainen, H., and Kulmala, M.: The Role of Sulfuric Acid in Atmospheric Nucleation, Science, 327, 1243–1246, https://doi.org/10.1126/science.1180315, http://science.sciencemag.org/content/327/5970/1243, 2010.

Stark, H., Yatavelli, R. L., Thompson, S. L., et al.: Methods to extract molecular and bulk chemical information from series of complex mass spectra with limited mass resolution, International Journal of Mass Spectrometry, 389, 26 – 38, https://doi.org/https://doi.org/10.1016/j.ijms.2015.08.011, http://www.sciencedirect.com/science/article/pii/S1387380615002626, 2015.

Svensmark, H., Enghoff, M. B., and Pedersen, J. O. P.: Response of cloud condensation nuclei ($>$ 50 nm) to changes in ion-nucleation, Physics Letters A, 377, 2343–2347, https://doi.org/10.1016/j.physleta.2013.07.004, 2013.

Zhang, R., Suh, I., Zhao, J., Zhang, D., Fortner, E. C., Tie, X., Molina, L. T., and Molina, M. J.: Atmospheric New Particle Formation Enhanced by Organic Acids, Science, 304, 1487–1490, https://doi.org/10.1126/science.1095139, http://science.sciencemag.org/content/304/5676/1487, 2004.

Experimental study of H_2SO_4 aerosol nucleation at high ionization levels

Maja Tomicic [1], Martin Bødker Enghoff [1], and Henrik Svensmark [1]

[1]National Space Institute, Danish Technical University, Elektrovej 327, Kgs. Lyngby, Denmark

Abstract. One hundred and ten direct measurements of aerosol nucleation rate at high ionization levels were performed in an 8 m^3 reaction chamber. Neutral and ion-induced particle formation from sulphuric acid (H_2SO_4) as a function of ionization and H_2SO_4 concentration was studied. Other species that could participate in the nucleation, such as NH_3 or organic compounds, were not measured ~~. The measurements extend the parameter space of measurements described by Dunne et al. (2016) (at T=295 K and RH=38%) by expanding to lower~~ but assumed constant and the concentration was estimated based on the parametrization by Gordon et al. (2017). Our parameter space is thus: [H_2SO_4 ~~concentrations (~~]=$4 \cdot 10^6$ - $3 \cdot 10^7$ cm^{-3} ~~) and higher ion concentrations (~~, [NH_3+ org]=2.2 ppb, T=295 K, RH=38%, and ion concentrations of 1700 - 19000 cm^{-3} ~~)~~. The ion concentrations, which correspond to levels caused by a nearby supernova, were achieved with gamma ray sources. Nucleation rates were directly measured with a particle size magnifier (PSM Airmodus A10) at a size close to critical cluster size (mobility diameter of ∼1.4 nm) and formation rates at mobility diameter of ∼4 nm were measured with a CPC (TSI model 3775). The measurements show that nucleation increases by around ~~a factor of five~~ an order of magnitude when the ionization increases from background to supernova levels under fixed gas conditions. The results expand the parametrization ~~from Dunne et al. (2016)~~ presented in Dunne et al. (2016) and Gordon et al. (2017) (for [NH_3+org]=2.2 ppb and T=295 K) to lower sulphuric acid concentrations and higher ion concentrations. The results make it plausible to expand the parametrization presented in Dunne et al. (2016) and Gordon et al. (2017) to higher ionization levels.

1 Introduction

Secondary aerosol particles, that are formed by nucleation processes in the atmosphere, play an important role in atmospheric chemistry and in Earth's climate system. They affect Earth's radiation balance by scattering solar radiation back to space and can also act as cloud condensation nuclei (CCN) and thereby affect the amount and radiative properties of clouds. Clouds have a net cooling effect on Earth's radiation budget of about -27.7 W m^{-2} (Hartmann, 1993). Thus, a small change in cloud properties can have significant effect on the climate system. Results by e.g Merikanto et al. (2009) and Yu and Luo (2009) have shown that a significant fraction (ranging between 31-70%) of cloud-forming aerosol particles in the atmosphere are secondary particles that originate from nucleation. Therefore, understanding nucleation is crucial in order to fully understand the atmospheric and climatic effects of aerosols.

Sulphuric acid (H_2SO_4) is the primary ingredient in the production of secondary aerosols because of its low vapor pressure and its ability to bond with water, which is ubiquitous in the atmosphere (Curtius, 2006). H_2SO_4 is primarily produced in the atmosphere from sulphur dioxide (SO_2) via oxidation by the OH radical, produced photochemically with ultraviolet light coming from the Sun. When H_2SO_4 collides with other molecules, it starts forming small clusters of molecules that can grow into new stable aerosols. If only H_2O and H_2SO_4 take part, the process is termed binary homogeneous nucleation. Nucleation can be significantly enhanced by other substances, the dominant ones being ammonia (NH_3) and organic molecules ~~(Kirkby et al., 2011; Dunne et al., 2016)~~(Zhang et al., 2004; Kirkby et al., 2011; Ehn et al., 2014; Dunne et al., 2016; Kirkby et al., 2016) . These processes are termed ternary and organic-mediated nucleation, respectively. Recent results show that in low H_2SO_4 environments nucleation also happens by condensation of highly oxygenated organic molecules alone (Bianchi et al., 2016). Further, ions enhance the nucleation process by stabilizing the molecular clusters, this process is termed ion-induced nucleation. The fraction of ion-induced nucleation of total particle formation was observed in various environments by Manninen et al. (2010). This study found that the fraction was in the range 1-30% being the highest in environments with generally low nucleation rates.

~~Typical~~ The typical concentration range of gas-phase H_2SO_4 in the atmosphere is $10^6 - 10^7$ cm^{-3}. The concentrations vary with location, time of the day and ~~outlet~~ emission of SO_2, which can be both anthropogenic and natural. Ions are ubiquitous in the lower atmosphere and are mainly produced by galactic cosmic rays (GCR), forming 1-40 ion pairs $\mathrm{cm}^{-3}\mathrm{s}^{-1}$. The formation rate depends on factors such as altitude, latitude, and the solar cycle. Ionization is higher above land than above ocean due to natural radioactivity from soils, and the maximum ionization is at altitudes of $\sim$ 13 km (Bazilevskaya et al., 2008). In addition to the natural variations in ionization, an event such as a nearby supernova would significantly increase the atmospheric ionization in the time following the event. There exists strong indications of a supernova at a relatively close distance of $\sim$50 pc from the solar system $\sim$ 2.2 million years ago (Knie et al., 2004; Kachelrieß et al., 2015; Savchenko et al., 2015; Fimiani et al., 2016). According to Melott et al. (2017) the increase in GCR from such an event would cause an increase in tropospheric ionization of up to a factor of 50 during the first few hundred years following the event.

Few measurements exist that quantify parameters affecting and assisting nucleation ~~(Berndt et al., 2006; Benson et al., 2011; Sipila et al.~~ (e.g. Berndt et al., 2006; Svensmark et al., 2007; Sipilä et al., 2010; Benson et al., 2011; Kirkby et al., 2011; Enghoff et al., 2011; Yu et al. . Recent laboratory measurements ~~by Dunne et al. (2016) determined~~ made in the European Organization for Nuclear Research CLOUD (Cosmics Leaving Outdoor Droplets) chamber were presented in Dunne et al. (2016) and showed the dependence on temperature, trace gas and ion concentrations~~and provided~~ . Based on the measurements a parametrization that can be incorporated into climate models was developed and this parametrization was improved by Gordon et al. (2017). These and other measurements, ~~(e.g., Svensmark et al., 2007; Enghoff et al., 2011; Kirkby et al., 2011)~~ (e.g. Svensmark et al., 2007; Enghoff et al., 2011; Kirk have verified that ionization helps the nucleation process. In this work we expand on these results by measuring nucleation at ion production rates (q) ranging from background levels to 560 $\mathrm{cm}^{-3}\mathrm{s}^{-1}$, corresponding to those following a nearby supernova, and atmospherically relevant H_2SO_4 concentrations ($4 \cdot 10^6$ - $3 \cdot 10^7$ cm^{-3}).

2 Experimental methods

The measurements presented in this work were performed in an 8 m^3 reaction chamber (SKY2). The setup is shown schematically in Fig. 1. The chamber is made of electro-polished stainless steel and has one side fitted with a Teflon foil to allow UV light (253.7 nm) to illuminate the chamber and start the photo-chemical reaction to generate H_2SO_4. ~~The chamber was continuously flushed at a rate of 25 L min^{-1}.~~ Dry purified air ~~and water vapor was added to~~ (20 L/min) from a compressor with an active charcoal, citric acid, and particle filter was passed through a humidifier and added to the chamber to reach a relative humidity of 38%. ~~Ozone (O_3), and sulphur dioxide (SO~~5 L/min of dry air from the same compressor went through an ozone generator where O_2 is photolyzed by a UV lamp to produce O_3 . Sulphur dioxide (3.5 mL/min) was added ~~to the chamber and the concentration~~ from a pressurized bottle (5 ppm SO_2 in air, AGA). The resulting concentrations of O_3 ~~was measured with~~ (20-30 ppb) and SO_2 (0.6-0.9 ppb) were measured by a Teledyne T400 analyzer and ~~SO_2~~ with a Thermo 43 CTL analyzer, respectively. The H_2SO_4 concentration was measured with a ~~chemical ionization atmospheric pressure interface time-of-flight~~ Chemical Ionization Atmospheric Pressure Interface Time-of-Flight (CI-API-ToF) mass spectrometer (Jokinen et al., 2012). The chamber is also equipped with instruments to measure temperature, differential and absolute pressure, humidity, and UV intensity. The pressure was held at a ~~slight (~ 0.1~~ standard pressure of ~ 1 bar with a slight (0.1 mbar) overpressure relative to the surroundings, the temperature at 295 K and the UV intensity was varied as part of the experiments.

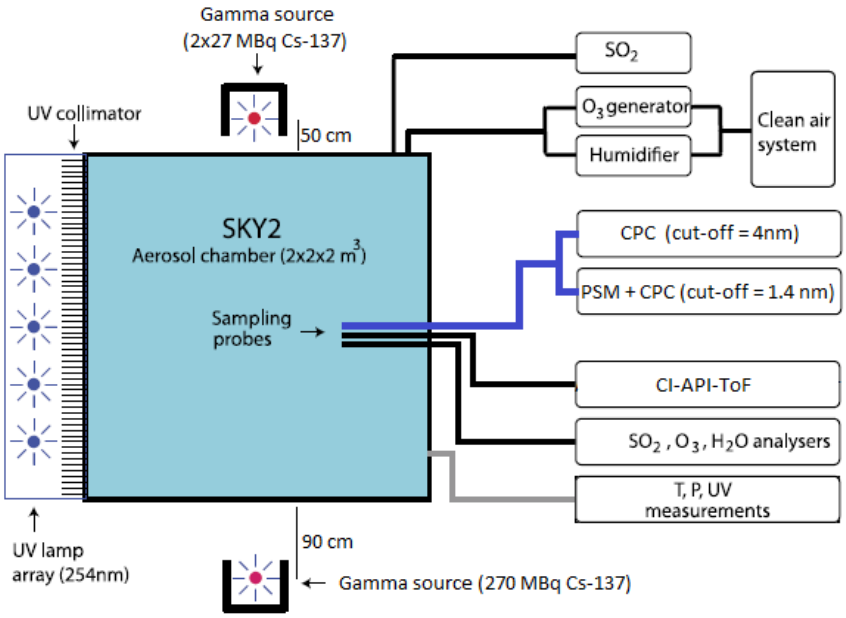

Figure 1. A schematic of the SKY2 reaction chamber and the instruments used for the experiment. The figure is an edited version of the schematic from Svensmark et al. (2013).

Two different condensation particle counters (CPCs) and a particle size magnifier (PSM) were used to count the aerosols formed in the experiments. A TSI model 3775 CPC was used to determine the aerosol particle concentration above a cutoff diameter of 4 nm ($d_{\mathrm{p,cutoff}}$ = 4 nm). And a TSI 3776 CPC ($d_{\mathrm{p,cutoff}}$ = 2.5 nm) was used in series with the PSM Airmodus A10, developed and described by (Vanhanen et al., 2011), to detect particles above a cut-off diameter of ∼1.4 nm. The cut-off diameter is defined as the mobility diameter of particles of which 50% are counted and it depends on the saturator flow rate and the chemical composition of the particles. For the PSM, the saturator flow rate was set to 1.3 L min^{-1} which corresponds to a cut-off diameter of 1.4 nm for tungstenoxide particles. The cut-off for H_2SO_4 aerosols is not known exactly. The cut-off diameter of the PSM is very close to the critical size of ∼1.5 nm (Kirkby et al., 2011) which allows for direct measurements of nucleation rate thereby avoiding extrapolations of the nucleation rate from larger sizes (Kürten et al., 2017). Both instruments (PSM and CPC) sampled from the same line and had identical sampling pathways as illustrated in Fig. 1. The CPC with the larger cut-off diameter was used on its own to achieve a larger size span between the instruments which enables the determination of the particle growth rate (GR).

2.1 Ionization of Air by Gamma Sources

The air in the 8 m^3 reaction chamber was ionized by gamma sources. Enghoff et al. (2011) have shown that the nature of the ionizing particles is not important for the nucleation of aerosols. Therefore, even though particles from an accelerator beam can have energies closer to GCR, gamma radiation, which is more accessible, can be used to study the ion-induced nucleation. Three Cs-137 sources were used in the setup; two 27 MBq and one 270 MBq. To achieve a homogeneous ~~radiation~~ irradiation of the chamber, the 270 MBq source was placed on one side of the chamber, at a ~ 90 cm distance, and the two 27 MBq sources were placed close to each other on the opposite side of the chamber, at ~ 50 cm distance. The setup is illustrated in Fig. 1. Ions are also produced in the chamber by naturally occurring GCR and background radiation from Radon at a rate of $\sim$ 3 $\mathrm{cm}^{-3}\mathrm{s}^{-1}$. In order to perform measurements at different ionization levels, lead shielding of varying thickness was placed in front of the sources. Four ionization levels were achieved by using either 0 cm, 1.5 cm, 3.5 cm, or 8.5 cm lead shielding.

The uniformity and level of the ionization caused by the sources was estimated from simulations in Geant 4, with the G4beamline program (CMS Groupware, 2017). Figure 2 shows the ionization rates (q) in the chamber caused by the gamma sources, for minimum and maximum shielding thickness. The graphs show the chamber as seen from opposite the UV lamps. Thus, the 270 MBq source is on the left side of the graphs. From the simulation results in Fig. 2, it is clear that when the gamma sources were fully exposed the 270 MBq source created more ion pairs than the two weaker sources on the opposite side of the chamber. The variation from highest to lowest ionization is around a factor of two which translates into a factor 1.4 in ion concentration. There is some circulation of the air in the chamber and the air is sampled from approximately in the middle between the sources as seen in Fig. 1, therefore it is assumed that the average ionization for the entire chamber is a good representation of the ionization of the sampled air.

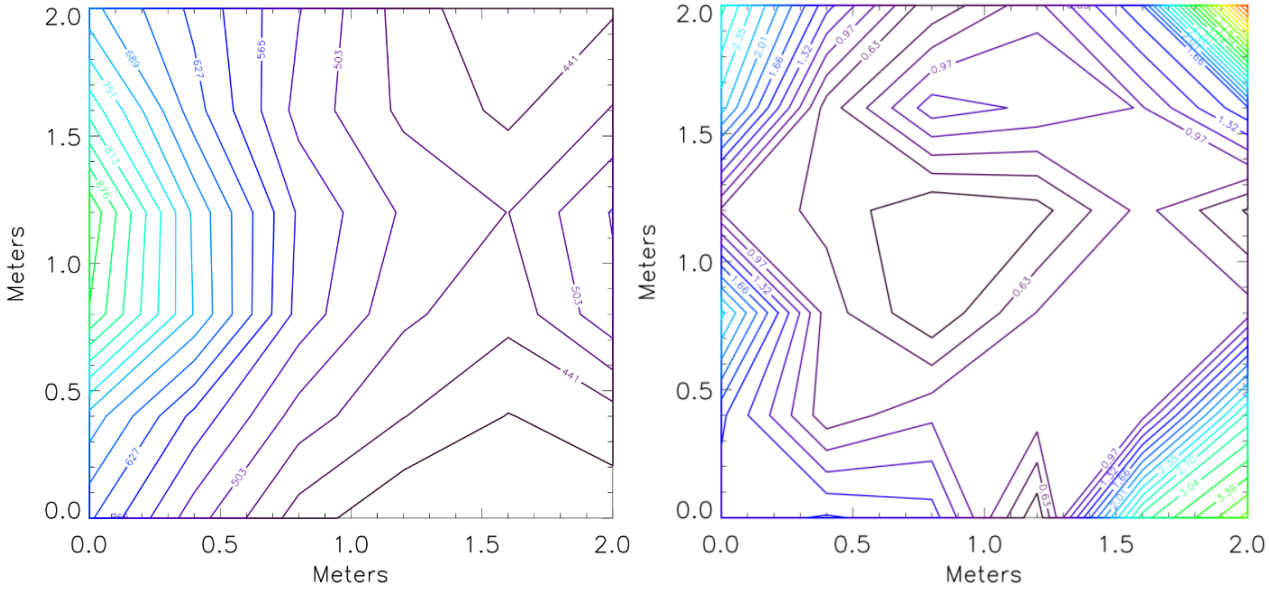

Figure 2. Geant 4 simulations of ionization rate, q [cm^{-3}s^{-1}], in the chamber with 0 cm (left) and 8.5 cm (right) lead shielding. The average ionization for the entire chamber is presented in Table 1.

Table 1. Average ionization rate for the entire chamber (q) achieved with the gamma sources at various ~~thickness~~ thicknesses of lead shielding calculated with Geant 4. ~~Ion density (~~N ~~)~~ is the ion density including the ions produced by naturally occurring radiation.

Shielding thickness	8.5 cm	3.5 cm	1.5 cm	0 cm
q [cm^{-3}s^{-1}]	1.4	10	109	560
N [cm^{-3}]*	1700	2900	8400	$1.9 \cdot 10^4$

* Approximate values calculated with $N = \sqrt{q_{\mathrm{total}}/\alpha}$, where α=1.6·10^{-6} is the recombination coefficient and q_{total} is the sum of the natural ionization (3 cm^{-3}s^{-1}) and the enhanced ionization caused by the sources.

2.2 Design of Experiments

The experiments were conducted by turning on the UV lamps for 20 minutes to generate H_2SO_4. The [H_2SO_4] depends on the intensity of the UV light, thus, by varying the intensity between experiments, the H_2SO_4 concentration was varied. Once sufficient H_2SO_4 was present, nucleation started and continued until the H_2SO_4 was used up and/or lost to the chamber walls. The aerosol formation rate was measured at the respective cut-off diameters with the PSM and CPC. The procedure lasted six to fourteen hours for a single run under fixed gas conditions, depending on the sulphuric acid concentration, because the system had to return to its initial conditions (PSM concentration < 2 cm^{-3}) before a new experiment was started. In between

experiments, the ionization conditions were varied by changing the amount of lead shielding in front of the gamma sources. At least one hour before each experiment the lead shielding was put in the right position to allow the ionization level to stabilize before the nucleation started.

The upper limit to the H_2SO_4 concentrations was chosen based on time constraints, because too high concentrations yielded a particle count which took a long time to decay back to initial conditions (< 2 cm^{-3}). The lower limit of the H_2SO_4 concentrations was chosen based on the particle detection limit of the ~~instrument. The CPC with cut-off diameter of 4 nm~~ CPC model 3775, which was the limiting instrument because the majority of the particles are lost during the growth from 1.4 to 4 nm. On average, 25% of the particles survive the growth. The survival is only 10% for low H_2SO_4 concentrations since the growth rate (GR) is slower in this case.

Every fifth measurement was performed as a reference experiment with a standard ion concentration (N = 2900 $cm^{-3}s^{-1}$) and UV intensity (20 %), to avoid unnoticed ~~drift~~ drifts in parameters or instruments. The reference experiments showed that the [H_2SO_4] varied despite of the identical UV setting because the O_3 concentration decreased during the measurement series. This drift was caused by the O_3 generator, in which a UV lamp was replaced immediately prior to the measurements series. The lamp intensity decreased with time causing smaller H_2SO_4 concentrations for a given UV setting. A list of settings and the number of measurements at each setting is presented in Table 2.

Table 2. The range of UV and radiation level settings that were varied through the measurement series. The radiation levels are: 0 : N = 1700 cm^{-3}, 1 : N = 2900 cm^{-3}, 2 : N = 8400 cm^{-3}, 3 : N = 19000 cm^{-3}. The last column shows the number of measurements at each setting. The reference measurements were performed at 20 % UV and radiation level 1.

UV intensity	Radiation level	# of Measurements
15 %	0/1/2/3	5/4/2/5
18 %	0/1/2/3	2/0/0/2
20 %	0/1/2/3	5/18/3/8
22 %	0/1/2/3	4/3/3/5
25 %	0/1/2/3	2/3/3/5
30 %	0/1/2/3	3/2/0/3
35 %	0/1/2/3	1/3/0/3
40 %	0/1/2/3	2/2/0/2
45 %	0/1/2/3	2/2/0/3

3 Data processing

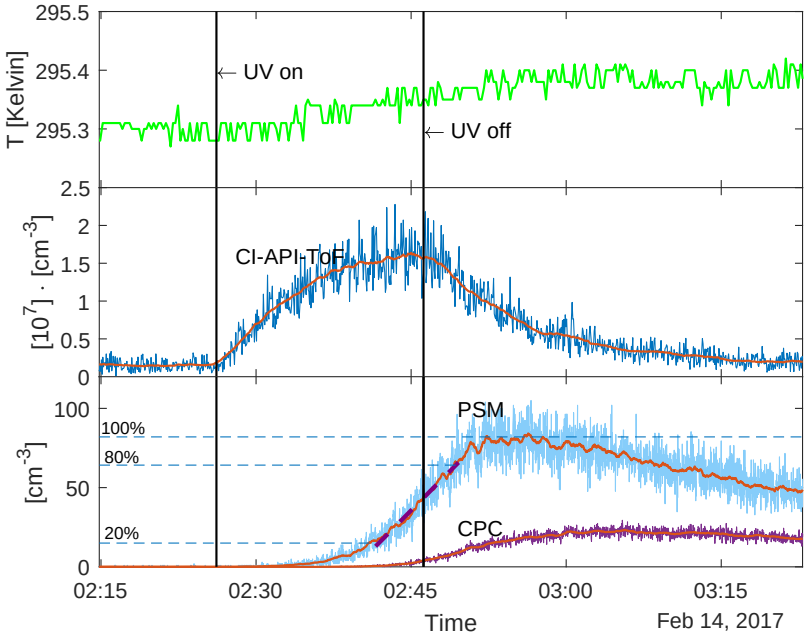

Figure 3. Run sequence for an experiment with 22% UV and N=8400 [cm^{-3}]. The vertical lines show when the UV lamps were turned on and off. Top panel: Temperature in the chamber. Middle panel: H_2SO_4 concentration measured with the CI-API-ToF and 50 point moving average shown in red. Bottom panel: Aerosol particle concentration measured with PSM and CPC (before the loss correction). The 50 point moving average is shown in red. The purple dashed line shows the linear fit between 20 and 80 of the maximum concentration. The gradient of this fit (made on the loss-corrected data) was used as the nucleation rate.

Figure 3 shows an example of a run sequence (for 22% UV and N=8400 [cm^{-3}]) as a function of time. The UV lamps were turned on for twenty minutes from 02:26:10 to 02:46:12. The top panel shows the temperature in the chamber during the experiment. It shows that the temperature increased by ~0.1 K when the UV lamps were turned on. When the UV was on the highest setting (45%) the temperature increased by 0.2 K. This slight increase in temperature is negligible in regards to the nucleation rate (5% change for a 0.2 K increase at the highest [H_2SO_4] based on Dunne et al. (2016)). Therefore, a constant temperature of 295.4 K was used in the further analysis. The second panel shows the H_2SO_4 concentration in units of 10^7 [cm^{-3}]. The red line is the 50 point boxcar moving average. Immediately after the UV lamps were turned on, the H_2SO_4 concentration started to increase. When the UV was turned off, the H_2SO_4 was lost to scavenging by aerosol particles and to the chamber walls. The third panel shows the aerosol particle concentration measured with the PSM and CPC without any corrections for the wall-losses. The red lines represent the 50 point boxcar moving average which is used for the further data analysis to avoid artefacts from noise. Corrections for particle loss to chamber walls are presented further down and the data analysis was performed on the corrected version of the moving average.

3.1 Sulphuric Acid Measurements

The CI-API-ToF mass spectrometer was used to determine the concentration of H_2SO_4. The CI-API-ToF spectrometer used in the setup was calibrated with the calibration system presented in Kürten et al. (2012). We use the calibration coefficient, C, as defined in Eq. (1) in Jokinen et al. (2012):

$$[\mathrm{H_2SO_4}] = \frac{\mathrm{HSO_4^-} + \mathrm{HSO_4^-} \cdot \mathrm{HNO_3}}{\mathrm{NO_3^-} + \mathrm{NO_3^-HNO_3} + \mathrm{NO_3^-(HNO_3)_2}} \cdot \mathrm{C} \quad (1)$$

The resulting calibration coefficient was C=$9.86 \cdot 10^9 \pm 4.22 \cdot 10^8$ molec cm^{-3}. Values in the literature vary from $5 \cdot 10^9$ to $1.89 \cdot 10^{10}$ molec cm^{-3} (Kürten et al., 2012).

The concentrations measured directly by the mass spectrometer are integrated concentrations of masses over a small region (± 0.5 AMU) of the spectrum. This means that the concentrations are overestimated because they include noise around the actual peak. This was also taken into account and corrected for using the results from ~~Hansen (2016)~~Hansen (2016) where the relation between analysis of the $\pm$ 0.5 AMU data from the API-ToF and data analyzed using Tofware (Stark et al., 2015) was found.

The ~~mean peak~~ H_2SO_4 concentration is determined ~~by using a~~ from the peak value of the 50 point ~~moving average. In~~ boxcar moving average (the red line in Figure 3). This method introduces a statistical uncertainty in addition to the uncertainty in the calibration factor~~there is a statistical uncertainty related to the determination of the mean peak concentration. This uncertainty~~. The statistical uncertainty arises from the fluctuations in the non-smoothed data and was ~~therefore~~ calculated from the standard error of the ~~mean of the~~ difference between the non-smoothed and the smoothed data for the 50 points around the peak.

The CI-API-ToF mass spectrometer broke down during the measurement series. Therefore, 60 out of 110 experiments do not include direct measurements of the H_2SO_4 concentration. For these experiments, the concentration was interpolated from a linear relation between the H_2SO_4 concentration, in the 50 direct measurements, and the GR of the aerosol particles, see Sect. 3.2. Previously, linear relations between GR and H_2SO_4 have been demonstrated by e.g., Kulmala et al. (2003).

3.2 Determination of Growth rate

The different cut-off diameters of the PSM A10 (1.4 nm) and TSI model 3775 CPC (4 nm) allow for a GR to be calculated from the time difference, Δt, between measurements in the two instruments. ~~We use a~~ A percentage limit (50% of the maximum concentration) was used instead of absolute numbers to take particle losses during growth into account. The difference in the cut-off diameters of the two instruments is 2.6 nm. The GR is therefore defined as:

$$GR = \frac{2.6\mathrm{nm}}{\Delta t} \quad (2)$$

The calculated GR were in the interval 14-34 nm h^{-1} at H_2SO_4 concentration ranging from $7.2{\cdot}10^6$ to $2.7 \cdot 10^7$ cm^{-3}. These GR values are reasonable compared to atmospheric GR ($\sim$ 1-20 nm^{-1}) (Kulmala et al., 2004). We note that although the GR are higher than expected from pure sulphuric acid condensation at the kinetic limit indicating the participation of other vapours in the early growth (Tröstl et al., 2016) we still find a linear relationship between sulphuric acid and the GR. These other vapours can also contribute to the observed nucleation rates (See Sect. 4 Results and Discussion).

3.3 Determination of Nucleation Rate

Nucleation rates, J_D, were measured at a mobility diameter of D $\sim$1.4 nm with the PSM A10. The particle diameter of 1.4 nm comes close to the critical cluster size and therefore the PSM allows for direct measurements of the nucleation rate. The PSM measures the concentration of particles with diameters above the cut-off, $N_{1.4}$.

The nucleation rate is defined as: ~~$J_{1.4} = dN_{1.4}/dt$ and~~ $J = dN/dt$ where $N = N_{1.4}/exp(-k \cdot t)$. Here k is a loss term that represents loss to chamber walls and t is the time after the particles reached the critical size. From Svensmark et al. (2013) we have the size-dependent loss term k which is an approximation of particle loss to the chamber walls:

$$k = \lambda / r_i^{\gamma} \tag{3}$$

The term γ is detemined experimentally, in Svensmark et al. (2013), to $\gamma = 0.69 \pm 0.05$ and $\lambda = 6.2 \cdot 10^{-4}$ $nm^{\gamma} s^{-1}$. The average radius r_i that the particles have at a certain time is given by the critical radius (0.7 nm), the growth rate, and the time they had to grow in, this is multiplied by 0.5 to get the average size:

$$r_i = 0.7nm + GR \cdot 0.5 \cdot \Delta t_i \tag{4}$$

The loss term is used to correct the particle count from the PSM at any time and the result is seen in Figure 4.

The nucleation rate $J_{1.4}$ was determined by calculating the gradient of the area between the 20% and 80% of each corrected peak of particle concentration. ~~Therefore, we use the standard deviation on the gradient as the one σ error on the nucleation rate.~~ This is illustrated by the dashed lines in Figure 3 and 4. The nucleation rates as a function of H_2SO_4 and ion concentrations are seen in Fig. 5 with ~~one σ~~ errorbars. The errorbars on the nucleation rate are the 95 % confidence interval of the gradient. The errorbars on the H_2SO_4 ~~and $J_{1.4}$~~ are the statistical standard errors. The Poisson counting uncertainty for the PSM ($\sqrt{N}$ (see Sect. 3.4)) and the calibration uncertainty for the mass spectrometer ($\sim 5\%$ measurement error + additional errors from calibration parameters ($\sim 30\%$, (Kürten et al., 2012))) are not shown.

3.4 Additional Uncertainties

Additional uncertainties in the particle concentration measurement arise, for example, from low particle counting statistics, from chemical composition dependent variation in the cutoff diameter of the particle counters, and from loss of particles in the sampling system. According to Kangasluoma and Kontkanen (2017) particle sampling and counting is a Poisson process and

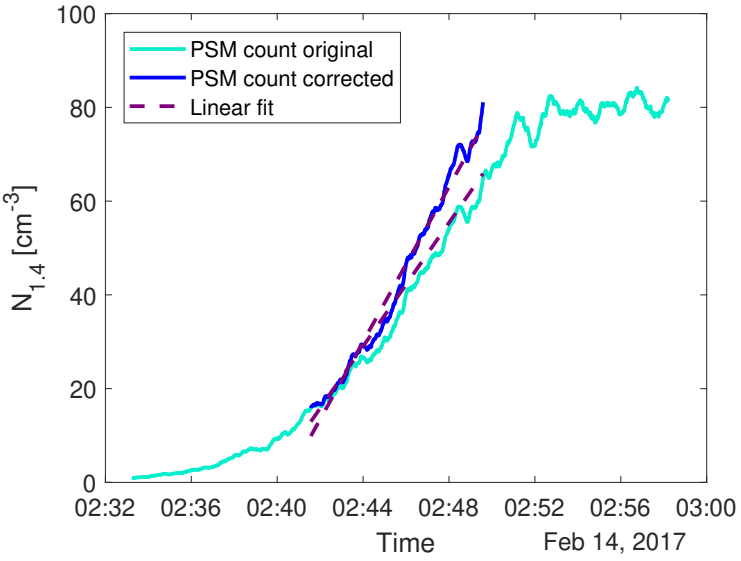

Figure 4. An example of the particle count from the PSM (light blue) and the loss corrected data (dark blue). The dashed line show the linear fit between 20 % and 80% of the maximum count. The gradient of the fit on the corrected data was used as the nucleation rate $J_{1.4}$.

the statistical uncertainty is determined from the Poisson counting uncertainty, $\sqrt{N}$, which describes the standard deviation, σ, of the counted particles, N.

Aerosols are lost to the walls of the sampling system due to diffusion. This type of loss is size dependent and was estimated using the Particle Loss Calculater (PLC) developed by von der Weiden et al. (2009). The loss function estimates that the losses of the 1.4 nm particles in the sampling system are $\sim$50% and only $\sim$15% for the 4 nm particles. Since we do not measure the particle size distribution diffusion losses are not included directly in the data analysis. This means that we could have underestimated the concentration of the smallest aerosols and thereby the nucleation rates.

4 Results and Discussion

~~To quantify the nucleation we adopt the parametrization presented in Dunne et al. (2016) and thus represent the nucleation~~ As the measurements presented here are an extension to the measurements presented in Dunne et al. (2016), at the given conditions, it is natural to compare the two. Therefore, results shown in Figure 5, are compared to the parametrization given in Gordon et al. (2017), which presents the parametrization of the CLOUD experiments to highest precision. In their work nucleation is represented as a sum of binary (b), ternary (t), neutral (n), ion-induced (i), and organic nucleation (org). The term representing the organic nucleation rate is not used ~~, as this~~ in the following, as our study does not intentionally add or measure

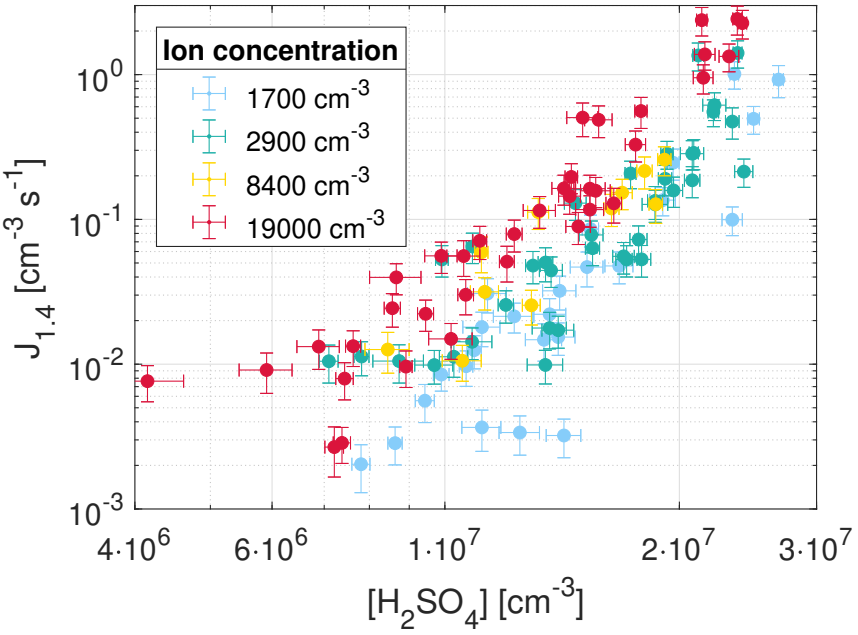

Figure 5. Nucleation rates as a function of sulphuric acid concentration and ion concentration. The errorbars represent one σ standard deviation on the [H_2SO_4] and the 95% CI on the nucleation rate.

organic molecules. ~~Atmospheric concentrations of methane are expected within the chamber but these are not expected to affect nucleation. There~~ Although, as deduced from the high GR, there might be traces of ~~other~~ organic species that can also contribute to the nucleation rate. The ~~concentrations are~~ concentration of organics is considered constant and ~~are~~ is included in the ternary nucleation rate~~to reduce the number of fitting parameters~~. Thus, a nucleation rate given by the sum of the four contributions is considered:

$$J = J_{b,n} + J_{t,n} + J_{b,i} + J_{t,i} \tag{5}$$

At the temperatures and gas concentrations used in this study ternary nucleation is expected to dominate as binary clusters are unstable (Hanson and Lovejoy, 2006). The model of binary nucleation presented in Ehrhart et al. (2016) shows good agreement with measurements performed in the European Organization for Nuclear Research CLOUD (Cosmics Leaving Outdoor Droplets) chamber at lower temperatures (<273 K). However at tropospheric temperatures (>273 K) the binary nucleation rate cannot explain the nucleation rates that are observed in either of these studies at the given sulphuric acid concentrations. Since the sulphuric acid concentration is lower in our study this is particularly important here. Ehrhart et al. (2016) attributes the differences to contamination which is more important in providing stabilization for the pre-nucleating clusters when the temperature and thereby evaporation is high. Nevertheless, we have included the binary term for the sake of completeness.

Ammonia (NH_3) is filtered from the air that enters the chamber with a citric acid filter. However, trace amounts (which can originate from incomplete filtering or introduction through the humidifier or the bottled SO_2 in air) are still present in the chamber and contribute to the production of stable clusters together with organic molecules. As the concentration ~~is not measured, the two ternary processes involving NH_3 are not directly fitted from the data. Instead, they are included in the modelling by assuming that the concentration of~~ of neither NH_3 ~~and~~ or organic molecules is ~~constant in all measurements. Thereby, it can be determined from a comparison of the results obtained in this study with the results from Dunne et al. (2016)~~ measured an ammonia equivalent concentration [NH_3 + org] that represents both species is estimated by comparing the results from the two studies under the same conditions (including T=295 K, RH=38%, and N=1700 cm^{-3}~~in both studies).~~).

Figure 6 shows the parametrization from ~~Dunne et al. (2016)~~ Gordon et al. (2017) (dashed lines) on top of the data from our experiments with the [NH_3~~concentration set at 3~~] concentration set to 5.5$\cdot 10^{10}$ cm^{-3} (~~1.2~~ 2.2 ppbv), for N=1700 cm^{-3} (left) and all ionization levels (right). Since [NH_3]=~~3~~5.5$\cdot 10^{10}$ cm^{-3} is the value that gives the best match between ~~data (see Fig. 6)~~ the data and the extrapolated parametrization ~~(dashed lines)~~ it is assumed to represent the concentration of NH_3 and organic species, [NH_3 + org]. Atmospherically observed NH_3 concentrations are typically at the sub-ppbv and ppbv level (Erupe et al., 2010; Nowak et al., 2006). Since the air is filtered before entering the chamber, we would expect a concentration that is lower than the atmospheric. Once again, this is an indication of the presence of other nucleation-enhancing species in our chamber.

We note that nucleation rates were reported for a mobility diameter of 1.7 nm in Dunne et al. (2016) meaning that the rates measured in this study should be slightly overestimated since we measure at a mobility diameter of $\sim$1.4 nm ~~.~~(see Sect. 2).

As seen from Fig. 6 the parametrization presented in ~~Dunne et al. (2016)~~ Gordon et al. (2017) matches the nucleation rates from this study, when extrapolated to the same region, especially at [H_2SO_4] $< 2 \cdot 10^7$ cm^{-3}. At higher values of [H_2SO_4] the nucleation rates from this study are higher than expected from the parametrization. The ~~disagreement is further quantified by fitting the nonlinear function in Eq. (5) to the experimental data from this study. The two terms that represent the binary nucleation are given by:~~

$$J_{b,n} = k_{b,n}(T)[H_2SO_4]^{p_{b,n}}$$

~~and~~

$$J_{b,i} = k_{b,i}(T) n_{-} [H_2SO_4]^{p_{b,i}}$$

~~Where $J_{b,n}$ is the binary neutral rate and $J_{b,i}$ is the binary ion-induced rate, with n_- being the negative ion concentration. In this study the temperature is not varied, therefore the coefficients $k(T)$ that account for the temperature dependence, are~~

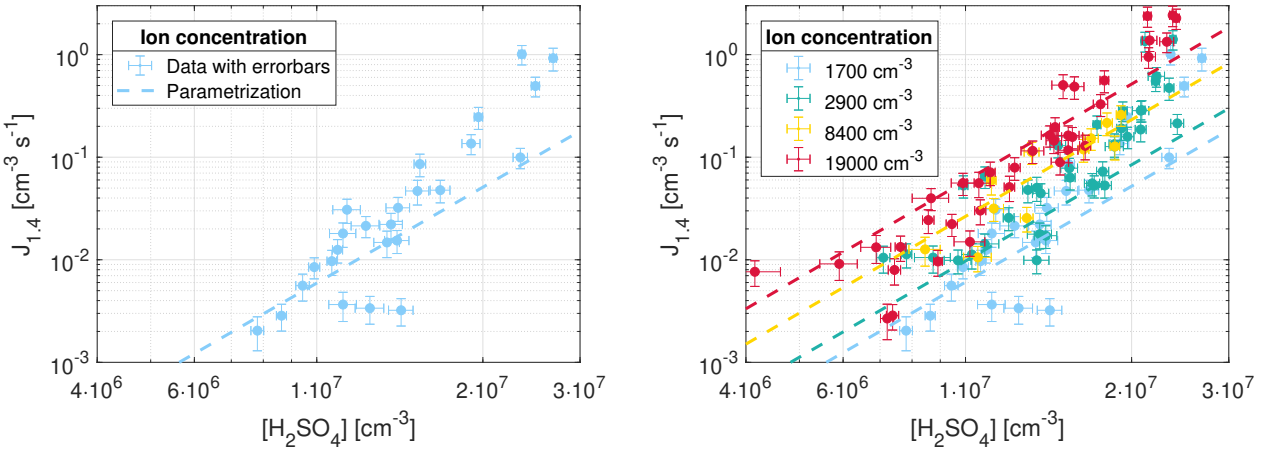

Figure 6. Parametrization from ~~Dunne et al. (2016)~~ Gordon et al. (2017) with [NH_3]=~~1.2~~ 2.2 ppb (dashed lines) and nucleation rate measurements from this study at T=295 K, RH=38%, N=1700 cm^{-3} (left) and all N (right).

~~constant and can also be calculated by extrapolation from Dunne et al. (2016, Sup. Mat.) to our region of H_2SO_4, N, T, and RH. Thus, we fit Eq. (5) to estimate the parameters $p_{b,n}$ and $p_{b,i}$ for high ionization levels.~~

~~The nonlinear fit was performed using a Levenberg-Marquardt algorithm in Matlab in order to find the best R^2 coefficient. The fit was weighted in order to include the standard deviation on the data. The best fit parameters are $p_{b,n} = 10.68$ and $p_{b,i} = 6.33$ for $J_{b,n}$ and $J_{b,i}$ respectively (R^2=0.77). Figure ?? shows the best fit parametrization and Table ?? lists all parameters.~~

~~Best fit of the parametrization to the experimental data. The parameters are presented in Table ??.~~

~~The second column presents the best fit parameters for neutral and ion-induced nucleation. The fit is performed with sulphuric acid and ammonia concentrations in units of 10^6 cm^{-3}. The third column shows the parameters from Dunne et al. (2016) for comparison. Parameters This study Dunne et al. (2016) $k_{b,n}$ * 4.79e-16 4.79e-16 $p_{b,n}$ 10.68 3.95 $k_{b,i}$ * 1.14e-13 1.14e-13 $p_{b,i}$ 6.33 3.37 The~~ resulting parametrization shows that at an atmospherically relevant H_2SO_4 concentration of $1 \cdot 10^7$cm^{-3} the increase in ions from background levels to the highest measured levels causes an increase in nucleation rate of around ~~a factor five~~ an order of magnitude.

The ~~slopes for Log $J_{1.4}$ vs. Log H_2SO_4 for fixed ion conditions, when only the binary term given by Eq. (4) is considered, were also calculated. The results are 5.1 ±0.3 for ionization level 0, 3.3 ±0.3 for level 1, 3.1 ±0.8 for level 2, and 4.7 ±0.3 for the highest ionization.~~

~~The~~ disagreement between the data and the expected parametrization could be caused by the narrow range of [H_2SO_4] in this study, which are all within one order of magnitude. Another explanation could be because the detection efficiency of the PSM is ~50% for particles close to the critical size of 1.4 nm. Since we use a percentage region instead of a fixed time interval when

calculating the nucleation rate (see Sect. 3.3), it is possible that the ~~parameters p and the slopes of Log J vs. Log~~ dependence on [H_2SO_4] ~~were~~ was overestimated due to the lower detection efficiency of PSM for particles smaller than 2 nm. At higher [H_2SO_4], more particles could grow into sizes that are detected more efficiently by the PSM compared to at lower [H_2SO_4]. This was taken into account by verifying that the regions between 20% and 80% of each peak of particle concentration were linear. If the detection efficiency was dependent on [H_2SO_4] these regions would not be linear but the gradient would increase with time for a given peak. However, we still note that the detection efficiency of the PMS could have affected the results in another way. Likewise, it is worth noting that the effect of ions on the detection efficiency of the PSM is unknown, but ions may be more efficiently detected (Winkler et al., 2008).

~~From the best fit of the parametrization, the exponent on the neutral nucleation rate, $p_{b,n}$, is higher than the ion induced, $p_{b,i}$. This suggest, as expected, that ions stabilize the clusters, suggesting that fewer H_2SO_4 molecules are needed to form a stable cluster when ions are present. When the experiments where fitted separately for each individual ion condition, the slope on the~~ It can be complicated to compare different experimental studies, even under similar conditions, because it is unclear how experimental techniques and parameters affect the results. Four studies (Kirkby et al., 2011; Almeida et al., 2013; Duplissy et al., 2016; Kü , all performed in the CLOUD chamber are most relevant for inter-comparison, because they were made in a reaction chamber analogous to this study. The experiments presented in Sipilä et al. (2010) were performed in a flow tube. Yet, we include these in the comparison, because in it nucleation was measured directly at the critical cluster size with a PSM instrument. Table 3 gives an overview of the studies and conditions that were compared. Some studies consist of several experiments using varying parameters. Table 3 only shows the measurements made under the conditions that were closest to the parameters of this study. The experiments from this study with lowest ionization are used for comparison, because this ionization level (4.4 cm^{-3} s^{-1}) is close to the cosmic ray background ionization (GCR $\sim$ 3 cm^{-3} s^{-1}).

Table 3. Comparison of similar nucleation rate experiments. The numbers refer to the different studies: 1: This study, 2: Kirkby et al. (2011) , 3: Almeida et al. (2013), 4: Duplissy et al. (2016), 5: Kürten et al. (2016) ,6: Sipilä et al. (2010). The fifth parameter, D, is the mobility diameter. GCR correspond to the background GCR (Galactic Cosmic Ray) ionization (~ 3 cm^{-3} s^{-1}). Cells with a - mean that the value was not measured or reported.

	1	2	3	4	5	6
H_2SO_4 [cm^{-3}]	$4 \cdot 10^6$ - $3 \cdot 10^7$	$2 \cdot 10^8$ - $1 \cdot 10^9$	$7 \cdot 10^6$ - $3 \cdot 10^8$	$5 \cdot 10^8$ - $8 \cdot 10^8$	$1 \cdot 10^8$ - $2 \cdot 10^8$	$2 \cdot 10^6$-$2 \cdot 10^8$
T [K]	295	292	278	299	292	293
RH	38%	38 %	38 %	36%	38%	22%
q [cm^{-3} s^{-1}]	4.4	GCR	GCR	GCR	GCR	GCR
D [nm]	1.4	1.7	1.7	1.7	1.7	$\sim 1.3 - 1.5$
NH_3	-	<35 ppt	2-250 ppt	-	1400 ppt	-†
J [cm^{-3} s^{-1}]*	0.002-1	0.005-30	0.003-25	0.01 - 1	3-10	1-1000

* The nucleation rates were read of the figures in the respective papers and are therefore only approximate values. † The observed growth rate in this study was close to that from pure sulphuric acid.

From Table 3 it is clear that experiments conducted under the exact same conditions as in this study do not exist. Nevertheless, the ~~small range of~~ nucleation rates in this study lie slightly below or within the range of the nucleation rates obtained in the experiments performed in the CLOUD chamber (studies 2-5). Except for study 3, which was made under lower temperatures, these studies have one to two orders of magnitude higher sulphuric acid concentrations ~~.~~

~~Figure ?? shows the individual contributions (from Eq. (5)) to the total nucleation rate for ionization level 1. From this we see that high values of the two p-exponents resulting from the fit (second column in Table ??), compared to results from Dunne et al. (2016) (third column in Table ??), can be explained mathematically by the fact that the ternary terms describes most of the nucleation and we therefore only fit the steep increase in nucleation rate for~~ than is the case for this study. As with the parametrization this indicates the existence of other nucleating species within our chamber. By comparing study 2 and 5 made under almost identical conditions the effect on nucleation of an increase in NH_3 concentration is evident (e.g at $[H_2SO_4] > 2 \cdot 10^7 = 2 \cdot 10^8$ cm^{-3} ~~.Individual contributions ($J_{b,n}$, $J_{b,i}$, $J_{t,n}$ and $J_{t,i}$) to the total nucleation rate ($J_{1.4}$), for ionization level 1.~~ $^{-3}$ which is the lower limit for study 2 and the upper limit for study 5).

The temperature used in this paper is only relevant to the boundary layer of the troposphere. At this high temperature evaporation of pre-nucleation clusters is very important and the stabilization provided by ions can have a strong effect (Lovejoy et al., 2004) as is also seen in this study. Higher in the troposphere where temperatures are lower the importance of evaporation decreases. However ions can still have a strong effect on the nucleation rates. Kirkby et al. (2011) showed that ions can affect pure binary nucleation rates at mid-troposphere conditions (~250 K). An even higher increase in ionization, as used in this work, would increase the nucleation rates even more - by about one order of magnitude according to the parametrization used here. The

concentrations of ternary gases is also expected to be lower in the free troposphere, which increases the effect of the ions.

In order to fully account for the variables in nucleation processes observed in this study, direct measurement of NH_3 and organic substances would have been preferred. Nonetheless, the results show that the nucleation increases linearly with ion concentration even at the highest ionizations. Also, a consistency with the results from Dunne et al. (2016) and Gordon et al. (2017) is shown.

5 Conclusions

The nucleation of H_2SO_4/H_2O aerosols was studied under near-atmospheric conditions in an 8 m^3 reaction chamber. Sulphuric acid was produced in situ in the range [H_2SO_4]= $4 \cdot 10^6$ - $3 \cdot 10^7$ cm^{-3} and the ionization of the air in the chamber was increased from background levels of $\sim$ 4 $cm^{-3}s^{-1}$ up to 560 $cm^{-3}s^{-1}$ (ion concentrations = 1700 - 19000 cm^{-3}) using gamma sources. Such levels of ionization are relevant for e.g. a nearby ($\sim$ 50 pc) supernova which is thought to have occurred $\sim$2.2 million years ago. The experiments were performed at T=295 K and RH=38%. The study shows that nucleation increases linearly with ion concentration, over the full range of ion concentrations. And, we find that nucleation increases by ~~a factor of five~~an order of magnitude, when the ion concentration is increased from background to maximum levels. ~~Further, the dependence of the nucleation rate on $H_2SO_4$is in the range 3-5 when only the binary nucleation rate is considered. This dependency could be overestimated because of the narrow range of H_2SO_4which is within one order of magnitude.~~ We have not measured the concentration of other nucleating species than sulphuric acid~~.~~, so the nucleation pathways are unclear. Based on comparisons with other studies we do conclude that ternary nucleation involving ammonia or organics is required to explain the observed nucleation rates. Still, this study is a novel contribution to the experimental studies of nucleation rates for the ammonia/organic-mediated H_2SO_4/H_2O system because of the direct measurements of nucleation rates at sizes close to the critical cluster size at high ion concentrations. This work expands the measurements presented in Dunne et al. (2016) for [NH_3+org]=2.2 ppb, RH=38% and T=295 K. Based on the presented experiments we find it ~~reasonable~~ plausible to expand the parametrization from ~~Dunne et al. (2016) to lower sulphuric acid concentrations and~~ Gordon et al. (2017) to higher ion concentrations.

Data availability. The datasets generated and analysed during the current study are available from the corresponding author on request.

Author contributions. M. Tomicic co-designed and co-performed the experiments, performed the data analysis and co-wrote the paper. M. B. Enghoff co-designed and co-performed the experiments and provided input to the data analysis and co-wrote the paper. H. Svensmark provided input to all parts of the work.

Competing interests. The authors declare no competing interests.

Acknowledgements. We thank Mikael Jensen and DTU NUTECH for lending us the 270 MBq Cs-137 source and for help with the transport. We thank Andreas Kürten for lending us his model for the calibration of the CI-API-ToF. We thank Knud Højgaards Foundation for funding the TSI 3776 CPC.

References

Almeida, J. et al.: Molecular understanding of sulphuric acid–amine particle nucleation in the atmosphere, Nature, 502, https://doi.org/doi:10.1038/nature12663, 2013.

Bazilevskaya, G. A., Usoskin, I. G., Flückiger, E. O., et al.: Cosmic Ray Induced Ion Production in the Atmosphere, Space Science Reviews, 137, 149–173, https://doi.org/10.1007/s11214-008-9339-y, https://doi.org/10.1007/s11214-008-9339-y, 2008.

Benson, D. R., Yu, J. H., Markovich, A., and Lee, S.-H.: Ternary homogeneous nucleation of H_2SO_4, NH_3, and H_2O under conditions relevant to the lower troposphere, Atmospheric Chemistry and Physics, 11, 4755–4766, https://doi.org/10.5194/acp-11-4755-2011, https://www.atmos-chem-phys.net/11/4755/2011/, 2011.

Berndt, T., Böge, O., and Stratmann, F.: Formation of atmospheric H2SO4/H2O particles in the absence of organics: A laboratory study, Geophysical Research Letters, 33, n/a–n/a, https://doi.org/10.1029/2006GL026660, http://dx.doi.org/10.1029/2006GL026660, l15817, 2006.

Bianchi, F., Tröstl, J., Junninen, H., et al.: New particle formation in the free troposphere: A question of chemistry and timing, Science, 352, 1109–1112, https://doi.org/10.1126/science.aad5456, http://science.sciencemag.org/content/352/6289/1109, 2016.

CMS Groupware: G4-Beamline open source software, http://www.muonsinternal.com/muons3/G4beamline, 2017.

Curtius, J.: Nucleation of atmospheric aerosol particles, Comptes Rendus Physique, 7, 1027 – 1045, https://doi.org/https://doi.org/10.1016/j.crhy.2006.10.018, http://www.sciencedirect.com/science/article/pii/S1631070506002301, nucleation, 2006.

Dunne, E. M., Gordon, H., Kürten, A., et al.: Global atmospheric particle formation from CERN CLOUD measurements, Science, 354, 1119–1124, https://doi.org/10.1126/science.aaf2649, http://science.sciencemag.org/content/354/6316/1119, 2016.

Duplissy, J., Merikanto, J., Franchin, A., Tsagkogeorgas, G., Kangasluoma, J., Wimmer, D., Vuollekoski, H., Schobesberger, S., Lehtipalo, K., Flagan, R., et al.: Effect of ions on sulfuric acid-water binary particle formation: 2. Experimental data and comparison with QC-normalized classical nucleation theory, Journal of Geophysical Research: Atmospheres, 121, 1752–1775, 2016.

Ehn, M. et al.: A large source of low-volatility secondary organic aerosol, Nature, 506, https://doi.org/doi:10.1038/nature13032, 2014.

Ehrhart, S., Ickes, L., et al.: Comparison of the SAWNUC model with CLOUD measurements of sulphuric acid-water nucleation, Journal of Geophysical Research: Atmospheres, 121, 12,401–12,414, https://doi.org/10.1002/2015JD023723, http://dx.doi.org/10.1002/2015JD023723, 2015JD023723, 2016.

Enghoff, M. B., Pedersen, J. O. P., Uggerhøj, et al.: Aerosol nucleation induced by a high energy particle beam, Geophysical Research Letters, 38, n/a–n/a, https://doi.org/10.1029/2011GL047036, http://dx.doi.org/10.1029/2011GL047036, l09805, 2011.

Erupe, M. E., Benson, D. R., Li, J., et al.: Correlation of aerosol nucleation rate with sulfuric acid and ammonia in Kent, Ohio: An atmospheric observation, Journal of Geophysical Research: Atmospheres, 115, n/a–n/a, https://doi.org/10.1029/2010JD013942, http://dx.doi.org/10.1029/2010JD013942, d23216, 2010.

Fimiani, L., Cook, D. L., Faestermann, T., Gómez-Guzmán, J. M., Hain, K., Herzog, G., Knie, K., Korschinek, G., Ludwig, P., Park, J., Reedy, R. C., and Rugel, G.: Interstellar ^{60}Fe on the Surface of the Moon, Phys. Rev. Lett., 116, 151 104, https://doi.org/10.1103/PhysRevLett.116.151104, https://link.aps.org/doi/10.1103/PhysRevLett.116.151104, 2016.

Gordon, H., Kirkby, J., Baltensperger, U., et al.: Causes and importance of new particle formation in the present-day and preindustrial atmospheres, Journal of Geophysical Research: Atmospheres, 122, https://doi.org/10.1002/2017JD026844, 2017.

Hansen, N.: Analysis of CI API-ToF mass spectrometer data from an atmospheric reaction chamber, Bachelor's thesis, National Space Institute, Danish Technical Univertsity, Denmark, 2016.

Hanson, D. R. and Lovejoy, E. R.: Measurement of the Thermodynamics of the Hydrated Dimer and Trimer of Sulfuric Acid, The Journal of Physical Chemistry A, 110, 9525–9528, https://doi.org/10.1021/jp062844w, https://doi.org/10.1021/jp062844w, pMID: 16884184, 2006.

Hartmann, D. L.: Radiative effects of clouds on earth's climate, in: Aerosol–Cloud–Climate Interactions, edited by Hobbs, P. V., vol. 54, pp. 151–173, Academic Press, 1993.

Jokinen, T., Sipilä, M., Junninen, H., et al.: Atmospheric sulphuric acid and neutral cluster measurements using CI-APi-TOF, Atmospheric Chemistry and Physics, 12, 4117–4125, https://doi.org/10.5194/acp-12-4117-2012, http://www.atmos-chem-phys.net/12/4117/2012/, 2012.

Kachelrieß, M., Neronov, A., and Semikoz, D. V.: Signatures of a Two Million Year Old Supernova in the Spectra of Cosmic Ray Protons, Antiprotons, and Positrons, Phys. Rev. Lett., 115, 181 103, https://doi.org/10.1103/PhysRevLett.115.181103, https://link.aps.org/doi/10.1103/PhysRevLett.115.181103, 2015.

Kangasluoma, J. and Kontkanen, J.: On the sources of uncertainty in the sub-3nm particle concentration measurement, Journal of Aerosol Science, 112, 34 – 51, https://doi.org/https://doi.org/10.1016/j.jaerosci.2017.07.002, http://www.sciencedirect.com/science/article/pii/S002185021730054X, 2017.

Kirkby, J., Curtius, J., Almeida, J., Dunne, E., et al.: Role of sulphuric acid, ammonia and galactic cosmic rays in atmospheric aerosol nucleation, Nature, 476, 429–433, https://doi.org/10.1038/nature10343, 2011.

Kirkby, J., Duplissy, J., Sengupta, K., et al.: Ion-induced nucleation of pure biogenic particles, Nature, 533, https://doi.org/doi:10.1038/nature17953, 2016.

Knie, K., Korschinek, G., Faestermann, T., Dorfi, E. A., et al.: ^{60}Fe Anomaly in a Deep-Sea Manganese Crust and Implications for a Nearby Supernova Source, Phys. Rev. Lett., 93, 171 103, https://doi.org/10.1103/PhysRevLett.93.171103, http://link.aps.org/doi/10.1103/PhysRevLett.93.171103, 2004.

Kürten, A., Bianchi, F., Almeida, J., et al.: Experimental particle formation rates spanning tropospheric sulfuric acid and ammonia abundances, ion production rates, and temperatures, Journal of Geophysical Research: Atmospheres, 121, 12,377–12,400, https://doi.org/10.1002/2015JD023908, http://dx.doi.org/10.1002/2015JD023908, 2015JD023908, 2016.

Kulmala, M., Dal Maso, M., Mäkelä, J., Pirjola, L., et al.: On the formation, growth and composition of nucleation mode particles, 53, 479 – 490, 2003.

Kulmala, M., Vehkamäki, H., Petäjä, T., Maso, M. D., et al.: Formation and growth rates of ultrafine atmospheric particles: a review of observations, Journal of Aerosol Science, 35, 143 – 176, https://doi.org/https://doi.org/10.1016/j.jaerosci.2003.10.003, http://www.sciencedirect.com/science/article/pii/S0021850203004373, 2004.

Kürten, A., Rondo, L., Ehrhart, S., and Curtius, J.: Calibration of a Chemical Ionization Mass Spectrometer for the Measurement of Gaseous Sulfuric Acid, J. Phys. Chem. A, 116, 6375–6386, https://doi.org/doi:10.1021/jp212123n, 2012.

Kürten, A., Li, C., Bianchi, F., Curtius, J., et al.: New particle formation in the sulfuric acid-dimethy lamine-water system: Reevaluation of CLOUD chamber measurements and comparison to an aerosol nucleation and growth model, pp. 1–31, 2017.

Lovejoy, E. R., Curtius, J., and Froyd, K. D.: Atmospheric ion-induced nucleation of sulfuric acid and water, Journal of Geophysical Research (Atmospheres), 109, 1–11, https://doi.org/10.1029/2003JD004460, 2004.

Manninen, H. E., Nieminen, T., Asmi, E., Gagné, S., et al.: EUCAARI ion spectrometer measurements at 12 European sites – analysis of new particle formation events, Atmospheric Chemistry and Physics, 10, 7907–7927, https://doi.org/10.5194/acp-10-7907-2010, https://www.atmos-chem-phys.net/10/7907/2010/, 2010.

Melott, A. L., Thomas, B. C., Kachelrieß, M., Semikoz, D. V., and Overholt, A. C.: A Supernova at 50 pc: Effects on the Earth's Atmosphere and Biota, The Astrophysical Journal, 840, 105, http://stacks.iop.org/0004-637X/840/i=2/a=105, 2017.

Merikanto, J., Spracklen, D. V., Mann, G. W., Pickering, S. J., and Carslaw, K. S.: Impact of nucleation on global CCN, Atmospheric Chemistry and Physics, 9, 8601–8616, https://doi.org/10.5194/acp-9-8601-2009, https://www.atmos-chem-phys.net/9/8601/2009/, 2009.

Nowak, J. B., Huey, L. G., Russell, A. G., Tian, D., et al.: Analysis of urban gas phase ammonia measurements from the 2002 Atlanta Aerosol Nucleation and Real-Time Characterization Experiment (ANARChE), J. Geophys. Res., 111, https://doi.org/doi:17310.11029/12006JD007113, 2006.

Savchenko, V. et al.: Imprint of a 2 Million Year Old Source on the Cosmic-Ray Anisotropy, The Astrophysical Journal, 809, https://doi.org/https://doi.org/10.1088/2041-8205/809/2/L23, 2015.

Sipilä, M., Berndt, T., Petäjä, T., Brus, D., Vanhanen, J., Stratmann, F., Patokoski, J., Mauldin, R. L., Hyvärinen, A.-P., Lihavainen, H., and Kulmala, M.: The Role of Sulfuric Acid in Atmospheric Nucleation, Science, 327, 1243–1246, https://doi.org/10.1126/science.1180315, http://science.sciencemag.org/content/327/5970/1243, 2010.

Sipila, M., Berndt, T., Petaja, T., et al.: The Role of Sulfuric Acid in Atmospheric Nucleation, Science, 327, 1243–1246, https://doi.org/10.1126/science.1180315, http://www.sciencemag.org/cgi/doi/10.1126/science.1180315, 2010.

Stark, H., Yatavelli, R. L., Thompson, S. L., et al.: Methods to extract molecular and bulk chemical information from series of complex mass spectra with limited mass resolution, International Journal of Mass Spectrometry, 389, 26 – 38, https://doi.org/https://doi.org/10.1016/j.ijms.2015.08.011, http://www.sciencedirect.com/science/article/pii/S1387380615002626, 2015.

Svensmark, H., Pedersen, J. O. P., Marsh, N. D., Enghoff, M. B., and Uggerhøj, U. I.: Experimental evidence for the role of ions in particle nucleation under atmospheric conditions, Proceedings of the Royal Society A, 463, 385–396, 2007.

Svensmark, H., Enghoff, M. B., and Pedersen, J. O. P.: Response of cloud condensation nuclei (> 50 nm) to changes in ion-nucleation, Physics Letters A, 377, 2343–2347, https://doi.org/10.1016/j.physleta.2013.07.004, 2013.

Tröstl, J. et al.: The role of low-volatility organic compounds in initial particle growth in the atmosphere, Nature, 533, https://doi.org/doi:10.1038/nature18271, 2016.

Vanhanen, J., Mikkilä, J., Lehtipalo, K., Sipilä, M., et al.: Particle Size Magnifier for Nano-CN Detection, Aerosol Science and Technology, 45, 533–542, https://doi.org/10.1080/02786826.2010.547889, http://www.tandfonline.com/doi/abs/10.1080/02786826.2010.547889, 2011.

von der Weiden, S.-L., Drewnick, F., and Borrmann, S.: Particle Loss Calculator – a new software tool for the assessment of the performance of aerosol inlet systems, Atmospheric Measurement Techniques, 2, 479–494, https://doi.org/10.5194/amt-2-479-2009, https://www.atmos-meas-tech.net/2/479/2009/, 2009.

Winkler, P. M., Steiner, G., Vrtala, A., Vehkamäki, H., et al.: Heterogeneous Nucleation Experiments Bridging the Scale from Molecular Ion Clusters to Nanoparticles, Science, 319, 1374–1377, https://doi.org/10.1126/science.1149034, http://science.sciencemag.org/content/319/5868/1374, 2008.

Yu, F. and Luo, G.: Simulation of particle size distribution with a global aerosol model: contribution of nucleation to aerosol and CCN number concentrations, Atmospheric Chemistry and Physics, 9, 7691–7710, https://doi.org/10.5194/acp-9-7691-2009, https://www.atmos-chem-phys.net/9/7691/2009/, 2009.

Yu, H., Dai, L., Zhao, Y., et al.: Laboratory observations of temperature and humidity dependencies of nucleation and growth rates of sub-3 nm particles, Journal of Geophysical Research: Atmospheres, 122, 1919–1929, https://doi.org/10.1002/2016JD025619, http://dx.doi.org/10.1002/2016JD025619, 2016JD025619, 2017.

Zhang, R., Suh, I., Zhao, J., Zhang, D., Fortner, E. C., Tie, X., Molina, L. T., and Molina, M. J.: Atmospheric New Particle Formation Enhanced by Organic Acids, Science, 304, 1487–1490, https://doi.org/10.1126/science.1095139, http://science.sciencemag.org/content/304/5676/1487, 2004.